A novel method for the observation of membrane transporter dynamics

Lyle W. Horn
Department of Physiology, Temple University School of Medicine, Philadelphia, Pennsylvania 19140 USA

ABSTRACT A new method is proposed for measuring the dynamic properties of a membrane transporter by means of steady-state fluxes. Any voltage-sensitive transporter will give a flow of substrate in the presence of a steady-state periodic membrane potential. The periodic steady-state flow, averaged over one period, is a flux that can be measured by traditional steady-state techniques, such as the radioactive tracer method. The average flux, solely due to the periodic field, is described by a set of Lorentzian functions that depend on the applied periodic field amplitude and frequency. The normal mode amplitudes and frequencies of these Lorentzians are model-independent parameters of the transport mechanism. Measurement of the average flux as a function of the applied periodic frequency permits determination of system relaxation times as the reciprocals of the midpoints of the Lorentzian curves, which in turn can be used to estimate individual rate constants of specific models.

It was found by simulation of a six-state model of the electrogenic Na^+/glucose cotransporter, using published estimates of the model rate constants, that the periodic field effects can be large and rich with measurable details that can be used to study the mechanism thoroughly. The new method serves in this case to complement and expand on the information obtainable by means of the voltage clamp method. It was also found by means of simulations of a nonelectrogenic six-state cotransporter model that experimentally measurable effects are expected and that results can be used to distinguish among alternative kinetic models as well as to estimate individual rate constants. The range of dynamic information available with this method is not accessible by voltage clamp or other pre-steady-state methods presently in use.

INTRODUCTION

How can we obtain dynamic information about a mediated transport mechanism? Eigen and DeMaeyer (1) pioneered the application of perturbation theory to chemical reaction kinetics as a means for obtaining individual rate constants of complex kinetic mechanisms. Läuger's group (2) applied Eigen's concepts to ion carriers in cell membranes and pointed out that in principle there is sufficient information in the amplitudes and time constants of relaxation data to determine all the rate constants of a transport mechanism. They focused on time-dependent relaxations of the transporter and recognized that experimental data may not have sufficient resolution to identify all of the characteristic time constants of a mechanism. Recent theoretical articles (3, 4) have shown how transport relaxation data of limited time resolution might be analyzed in terms of rate equations simplified by assuming that only one or two reaction steps are much slower than all others. The approach at best can yield information only about those rate-controlling steps. The analysis is limited to 0-*trans* conditions, and the key assumptions may not be applicable in many systems. The most common method for measuring transporter transients is the voltage clamp technique. Many transporters may not be electrogenic, may not express in either their native cells or in model cells to levels sufficient for good electrical signal to noise ratios, or may have relaxation times that are too short for detection. Alternative methods for studying transporter dynamics are desirable that can complement or extend transient current measurement techniques. This article presents one alternative that may have broad application and may be easier to apply than the traditional voltage clamp method.

The new method requires only steady-state transport measurements, admitting use of even the inherently slow but easily applied tracer flux experiment. The transporter need not be electrogenic, but it is required that at least one step of the mechanism be sensitive to the membrane potential. Voltage sensitivity of nonelectrogenic systems may be due to high-field access sites for substrate binding or the existence of a dipole moment that changes with the conformation of the integral membrane protein (5, 6). The essential concept of this new approach is that the steady-state transport rate should be a function of the frequency of an applied, periodic membrane potential (6). Measured frequency response functions are characteristic of the mechanism, model independent, and can be used to determine all individual rate constants of specific kinetic models. It should be emphasized that, theoretically, the information contents of a pre-steady-state experiment and a frequency response experiment are identical. However, the frequency response method may yield superior results for some preparations. This work seeks to show that useful new information can be obtained with the method even for the extremely difficult case of a nonelectrogenic system and that such data can serve to both discriminate among very similar transport models and to define a specific one.

THEORY

General kinetics

Assume that we have a general transport mechanism with N different states of the transporter and M different substrates. Denote the probability of occurrence of any

0006-3495/93/01/281/09 $2.00

transporter state i by the mole fraction of that state C_i. The time dependence of carrier state probabilities is described by the set of N first-order differential equations:

$$\dot{C}_i = \sum_{j=1}^{N} (k_{ji}C_j - k_{ij}C_i), \quad i = 1, \ldots, N; \quad i \neq j, \qquad (1)$$

where $\dot{C}_i$ denotes the first derivative of C_i with respect to time, and k_{ij} is either a true first-order rate constant or a pseudo-first-order rate constant formed by subsuming substrate concentration for the transition from state i to state j. Application of the principle of conservation of transporter reduces Eq. 1 to $N - 1$ equations of the general matrix form (2):

$$\dot{C}_i + \sum_{k=1}^{N-1} A_{ik}C_k = Q_i, \quad i = 1, \ldots, N - 1, \qquad (2)$$

where the coefficients A_{ik} and the inhomogeneous terms Q_i are functions of only the rate constants k_{ij}. General analytic solutions of Eq. 2 are not possible, and numerical integration forward in time is extremely difficult and often not feasible. This article focuses on periodic steady states in which the general time-dependent form of Eq. 2 must be satisfied but where integration is not needed.

Any voltage-sensitive step of a transport reaction can be represented as an equivalent charge displacement through some fraction of the membrane dielectric (2, 5). The rate constant for a voltage-sensitive step is then expressed as:

$$k_{ij} = k^0_{ij} \exp\{-Z_{ij}F\Psi_m/RT\}, \qquad (3)$$

where Z_{ij} is the equivalent charge displaced through some fraction of the membrane dielectric for the transition from state i to state j, Ψ_m is the membrane potential, k^0_{ij} is the value of k_{ij} when $\Psi_m = 0$, F is Faraday's constant, R is the universal gas constant, and T is the absolute temperature.

It is assumed that the cell has a stable resting membrane potential in the absence of any applied periodic voltage that will be referred to as the "resting" or "DC" potential, Ψ_{DC}. It is assumed that a periodic potential of amplitude Ψ_{AC} and frequency ω can be superimposed experimentally. Solution of Eq. 2 will yield the state probabilities C_i as periodic functions of ω and Ψ_{AC} from which fluxes can be calculated. The steady-state flux, averaged over one period, will be a time-invariant quantity that is also a function of ω and Ψ_{AC} (7). Measurement of such fluxes as a function of ω can be compared with frequency responses predicted for specific kinetic models to evaluate the feasibility of the model and to estimate rate constants. Combined with DC steady-state experiments, in which fluxes are measured as functions of Ψ_{DC} and substrate concentrations, the dynamic experiments could yield reliable definitions of kinetic mechanisms in terms of the rate constants.

The range of dynamic experiments that is possible is large because frequency responses can be determined at different substrate concentrations and Ψ_{DC}. Varying substrate concentrations will affect pseudo-first-order rate constants only, whereas varying Ψ_{DC} will affect only voltage-sensitive rate constants. The frequency response will depend on all rate constants, so systematically varying a few at a time permits a sorting out of the reaction steps and more reliable estimates of specific constants under optimal conditions.

Application of theory

Astumian and Robertson (7, 8) analyzed cyclic reactions having an arbitrary number of states and utilized a small amplitude approximation to reach some powerful conclusions with practical application. The small amplitude approximation is that:

$$|Z_{ij}F\Psi_{AC}/RT| \equiv |\alpha_{ij}| < 1. \qquad (4)$$

The general periodic steady-state solution of Eq. 2 can be expressed as a Fourier series whose coefficients are functions of the α_{ij}. If the α_{ij} are small, then expansion of the Fourier coefficients in powers of α_{ij} permits all terms of the expansion of power > 2 to be ignored. This quadratic approximation will preserve most of the inherently nonlinear properties of Eqs. 2 and 3. The small amplitude restriction is not severe. The flux, averaged over one period, must be an even function of α_{ij} (8) so that the first neglected term in the quadratic approximation would be proportional to $\alpha^4_{ij}/64$, whereas the quadratic term would be proportional to $\alpha^2_{ij}/4$. Thus, if the largest $|\alpha_{ij}|$ were 0.9, then each neglected term of the series expansion would be <7% of the quadratic term. It should be noted that Eq. 4 is independent of the DC resting potential and that the Z_{ij} are unknown parameters that must be determined experimentally. It is not possible to know in advance whether Eq. 4 is satisfied during a frequency response experiment. The point can be checked directly, however, because the amplitude of the frequency-dependent part of the response must be proportional to Ψ^2_{AC} (8) if Eq. 4 holds. Such experiments also could be used to estimate the Z_{ij} (9).

The most important general conclusion derived from the small amplitude approximation is that the average flux from state i to state j, as a function of frequency, can be described by a sum of Lorentzians (8):

$$J_{ij} = J^\infty_{ij} + \sum_{k=1}^{N-1} \{B_{ij,k}/[1 + (\omega/\omega_k)^2]\}, \qquad (5)$$

where J^∞_{ij} is the average flux when the applied frequency ω is infinite, $B_{ij,k}$ are normal mode amplitudes proportional to Ψ^2_{AC} that depend on the k^0_{ij} and Z_{ij}, and the ω_k are the characteristic (or normal mode) frequencies of the mechanism determined solely by the k^0_{ij}. The ω_k are the eigenvalues of the coefficient matrix whose elements are A_{ij} in Eq. 2 (2, 5) and are the reciprocals of the relaxation time constants that might be detected in a pre-steady-state experiment. The $B_{ij,k}$ are determined from the row and column eigenvectors of the unitary diagonalization matrix for A_{ij} and the forcing functions Q_i (8). This conclusion is independent of any specific kinetic model so that Eq. 5 can be applied legitimately to any frequency response experiment satisfying the small amplitude restriction. The ω_k and $B_{ij,k}$ are general parameters that can be measured at different substrate concentrations and Ψ_{DC}'s. The number of normal modes that can be detected in any experiment will depend on the amplitude of each and the sensitivity of the flux measurements. However, unlike the pre-steady-state approach, this approach is independent of the instrumental time resolution because all fluxes are measured in the steady state. This report deals only with unidirectional isotopic tracer influxes, for which Eq. 5 is applied to the product release step of the mechanism.

The calculations in this article present the extra steady-state tracer influx in the presence of a periodic voltage as a percentage of the tracer influx at the DC resting potential (when both $\Psi_{AC} = 0$ and $\omega = 0$):

$$F_{ij} = 100[J_{ij}(\Psi_{AC} \neq 0)/J_{ij}(\Psi_{AC} = 0) - 1]. \tag{6}$$

It is easier to check the order of magnitude of the AC effect and to judge whether it can be measured reliably using F_{ij}, and the magnitude range for the AC effects in terms of F_{ij} will be the same for all possible experimental conditions. A decision about the significance of an AC effect can then be based on the accuracy with which the DC flux can be measured. $F_{ij} < 0$ indicates that the periodic field inhibits influx relative to the DC state, whereas $F_{ij} > 0$ indicates stimulation.

FREQUENCY RESPONSE OF A SIX-STATE TRANSPORTER

The electrogenic intestinal Na^+/glucose transporter is simulated first, using the model and rate constants reported by Parent et al. (10) to show that the new method can yield interesting and measurable results when applied to a well-known system. Then results are presented for a nonelectrogenic system to demonstrate the kinds of experimental data to be expected for a mechanism in which measurement of transporter current transients could be extremely difficult. A Fortran program was written to generate the small amplitude solutions of Eq. 2 according to the algorithm of Robertson and Astumian (8). The series expansion was taken to order α^2. The key step in the program involves the determination of the eigenvalues and eigenvectors of the coefficient matrix $\mathbf{A}_{ij}$. The flux frequency response can then be calculated directly from Eq. 5. Successful calculations require that the eigenvalues be determined to ≥60 bit precision because the matrix $\mathbf{A}_{ij}$ can be extremely stiff due to the large magnitude range of rate constants to be expected.

The computer program was tested in two ways. First, a simple four-state model was simulated. Program results were compared at each step of the algorithm with results of a manual calculation. The two calculations agreed to at least four significant figures. Second, the simulations of Liu et al. (11) of a four-state representation of the Na/K pump were reproduced to establish confidence that the implementation of the solution algorithm is equivalent to that of Astumian and collaborators. The reliability and accuracy of the small amplitude approximation was checked by comparing steady-state fluxes predicted by this method with those determined by numerical integration forward in time of Eq. 2. The periodic steady-state fluxes so predicted agreed to better than 10% when the parameter α was 0.5.

Case 1: the intestinal Na^+/glucose electrogenic cotransporter

Advantage has been taken of the high levels of expression of the rabbit intestinal Na^+/glucose cotransporter in *X. laevis* oocytes to observe transporter transients using electrical recording of transporter currents following voltage-clamp steps (12). Only one transporter relaxation could be detected due to a large capacity transient. The time constant ranged between 5 and 20 ms, depending on the Ψ_m. Transients could only be observed in the absence of the α-methyl-D-glucose (AMG) substrate. These experiments provided the first direct measurements of Na/glucose transporter transients and valuable information about the system time scale, although they were of limited scope and results could not be used for a deduction of system rate constants. However, careful use of both steady-state and transient data led Parent et al. (10) to propose a preliminary six-state transport model with rate constants for each state transition. The model can reproduce the transient data fairly well. It assumes that both Na ions bind before AMG, with mirror symmetry. The first Na binds extremely fast, so that the two first-order Na association steps can be combined into one second-order step. External Na binding and translocation of the empty carrier are voltage sensitive. The model is electrogenic.

The model of Parent et al. (10, 12) was used to simulate the frequency response of radioactive tracer AMG influx. Their model is presented in Fig. 1. The number of eigenvalues, ω_k, for this model is seven, including two for the tracer steps. Fig. 2 shows the predicted frequency responses of tracer AMG influx for DC steady-state experimental conditions similar to those used to derive the preliminary model. The first point to note is that the magnitudes of the responses are large and easily mea-

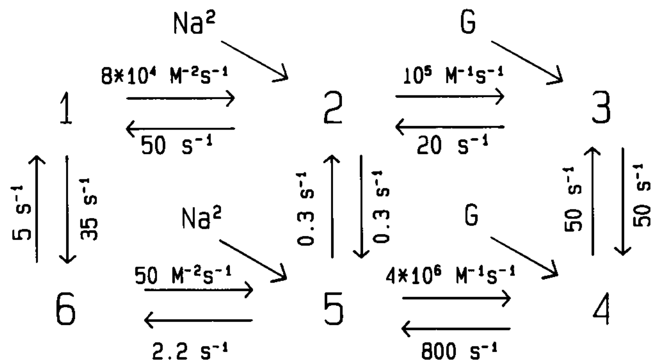

FIGURE 1 Six-state model of the intestinal Na^+/glucose cotransporter (Case 1) as defined in Fig. 2 of Parent et al. (10). The notation conforms to this work. True rate constants at $\Psi_{DC} = 0$ are specified next to each state transition. The (1, 6), (2, 5), and (3, 4) transitions are inward translocations. The voltage sensitivity parameters and all but two rate constants were taken directly from Parent et al. (10). The reported rate constants do not satisfy detailed balance, so k_{54}^0 was decreased 10-fold and k_{56}^0 was reduced from 10 to 2.19 s^{-1}. Rate constants on the *trans* side of the membrane were chosen for adjustment to ensure detailed balance because their published values have no direct experimental support and only 0-*trans* experiments were reported and simulated. The Na association rate is proportional to $[Na]^2$, so that the pseudo-first-order rate constant for this step would subsume this factor. It should be noted that the presence of a tracer of AMG requires the introduction of two additional states (7 and 8) to the diagram that are labeled with tracer. However, all true state transition rate constants for the tracer steps are identical to those for the native substrate. The tracer state connections are (2, 7), (7, 8), and (5, 8), which correspond to the unlabeled state connections (2, 3), (3, 4), and (5, 4). The usual assumption is made that the *trans* concentration of tracer AMG is zero.

sured. Depolarization enhances the response (Fig. 2 *A*). None is observable at $\Psi_{DC} = -50$ mV. At $\Psi_{DC} = 0$ mV, only one term in Eq. 5 would be required to describe the frequency response, with a normal mode frequency of 1.1 Hz (time constant 148 ms). Responses at +20 mV would require at least three normal mode frequencies in Eq. 5, namely 0.6, 7.1, and 17.8 Hz (time constants 249, 22.4, and 8.9 ms, respectively), whereas at $\Psi_{DC} = +50$ mV the three normal mode frequencies would be about the same as at +20 mV but the amplitudes would be increased.

The effects of external AMG and Na concentrations are shown in Fig. 2, *B* and *C*. Very large amplitude responses are seen at low substrate concentrations. When external AMG is 0.1 mM (Fig. 2 *B*), which is similar to the $K_{1/2}$ for these conditions (12), three normal modes are needed for Eq. 5 at 0.6, 3.8, and 218 Hz. Lowering AMG to 0.01 mM has little effect on the normal mode frequencies but enhances their amplitudes greatly. A similar pattern occurs when only external Na concentration is varied (Fig. 2 *C*). When the Na concentration is about one-half the Na $K_{1/2}$ (12), three normal modes might be observed at 0.6, 6.9, and 11.9 Hz, whereas reducing Na further serves mainly to increase the magnitudes of the normal modes.

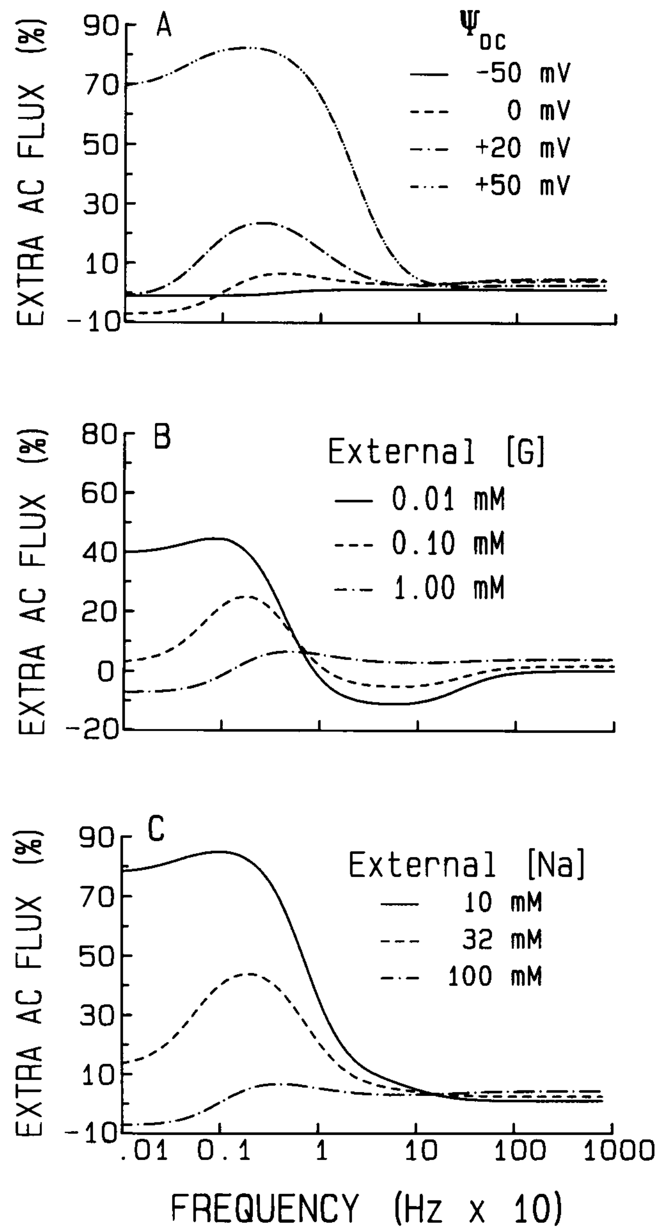

FIGURE 2 Frequency responses of the Na^+/glucose cotransporter model (Case 1) as specified in Fig. 1. The extra influx of tracer AMG due only to the periodic field is presented as a percent of the DC influx (Eq. 6). The frequency scale is logarithmic and is common to all three graphs. 0-*trans* substrate concentrations apply in all cases. Ψ_{AC} (32 mV) was chosen so that $|\alpha_{ij}|_{max} = 0.9$ (Eq. 4). Absolute influxes in the absence of a periodic electric field (DC influxes) were calculated assuming $5 \cdot 10^{10}$ carriers/oocyte and a surface area of 0.01 cm^2/oocyte (10). DC influxes are given for reference below and serve to define the 100% and 0% points of each curve. (*A*) Effect of the Ψ_{DC} for the conditions: $[Na]_0 = 100$ mM, $[AMG]_0 = 1.0$ mM. Proceeding from lowest to highest Ψ_{DC}, the absolute DC influxes would be 16.3, 11.5, 7.3, and 1.7 pmol/cm^2 s, respectively. (*B*) Effect of $[AMG]_0$ for the conditions: $\Psi_{DC} = 0$, $[Na]_0 = 100$ mM. Proceeding from lowest to highest $[AMG]_0$, the absolute DC influxes would be 0.9, 5.5, and 11.5 pmol/cm^2 s, respectively. (*C*) Effect of $[Na]_0$ for the conditions: $\Psi_{DC} = 0$, $[AMG]_0 = 1.0$ mM. Proceeding from lowest to highest $[Na]_0$, the absolute DC influxes would be 1.0, 5.7, and 11.5 pmol/cm^2 s, respectively.

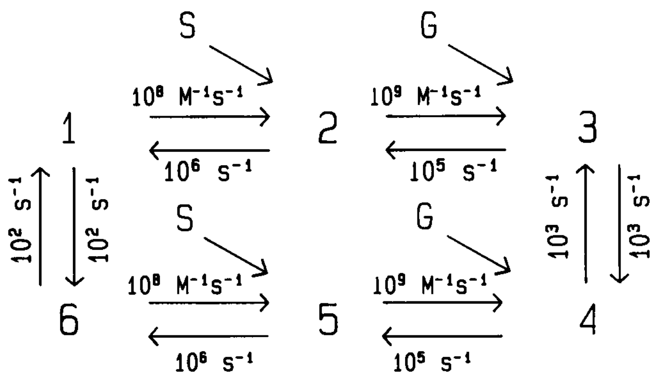

FIGURE 3 Six-state ordered binding model for substrates S and G. S-first binding with mirror symmetry is illustrated, but order and symmetry of substrate binding were varied (cf. text). True rate constants at $\Psi_{DC} = 0$ are given next to each state transition arrow. Any changes of rate constants are itemized in text. Step (1, 6) represents the inward translocation of empty carrier and step (3, 4) represents that of fully loaded carrier. The voltage sensitivity parameters Z_{ij} are specified for each specific case. Two extra states were introduced to account for the tracer of G, with state connections appropriate to each case. The *trans* concentration of the tracer of G was set to zero.

Nonelectrogenic six-state models

The kinetic mechanism is summarized in Fig. 3. It could represent an ordered binding cotransport system. Let the charges of substrates S and G be equal and opposite and the net charge on the transport protein be zero. Four variations of the model are possible based on substrate binding order and symmetry. This model is an extreme case where we might expect voltage effects to be minimal. It could not be studied in the DC steady state by observation of whole cell patch-clamp currents, and transient currents might be too small to distinguish from noise. The isotopic tracer flux method is the most feasible for measuring transport by this system. It is assumed that the translocation rate constants for the influx and efflux are equal and that the internal and external binding steps are symmetric when $\Psi_m = 0$. Translocation or substrate binding rate constant asymmetry can arise in this model when the resting $\Psi_{DC} \neq 0$, whereas different *cis* and *trans* substrate concentrations will produce asymmetry in the pseudo-first-order substrate association rate constants regardless of the Ψ_{DC}.

Rate constants shown in Fig. 3 were chosen to satisfy detailed balance and to ensure that substrate binding steps would be fast relative to membrane translocation steps. The translocation rate constant for the fully loaded carrier (k^0_{34}) was set much higher than most reported transporter turnovers. However, predicted normal mode frequencies can be adjusted by simple scaling if transporter turnover is slower and if all rate constants can be scaled uniformly. Rate constant scaling will have no effect on the predicted normal mode amplitudes. The magnitude of Z was chosen to be small when compared with highly voltage-sensitive structures such as a Na^+ channel gate with an effective charge parameter of +6 (13). The magnitude of Z is unimportant when considering the frequency response since only the product $Z\Psi_{AC}$ will affect the response magnitude. If Z is very small, then the periodic voltage signal can be made as large as the experimental preparation will tolerate to obtain a $Z\Psi_{AC}$ product that will produce a measurable response. The magnitude of Z is important primarily in determining the effect of the DC resting potential on the rate constants.

Case 2: rapid equilibrium, ordered substrate binding

Rapid substrate binding is the traditional assumption of transport kinetics, although it has been questioned frequently in recent work (3, 4, 10, 14). Because only membrane translocation is "slow," we might experimentally observe only one normal mode frequency in the Lorentzian expression for the flux. All other normal modes would have very small amplitudes. The simulations support this prediction.

This case does not require the full power of the general analysis because it can be reduced to a simple two-state model provided the rapid equilibrium approximation is valid on the time scale of all experimental frequencies. Define the substrate equilibrium association constant for step ij (K_i) in terms of the true second-order rate constant for substrate association rather than the pseudo-first-order rate constant. Then Eq. 2 can be reduced to a single equation governed by a single time constant, or normal mode frequency ω_1, given by a model-specific expression that is the sum of two independent terms ($\omega_1 = f + r$). f is a function of *cis* concentrations only, whereas r is a function of *trans* concentrations only. It is instructive at this point to show substrate concentrations explicitly. The expression for the case of S-first binding with mirror symmetry (Fig. 3) is:

$$\omega_1 = \frac{k_{16} + k_{34}\dfrac{S_o G_o}{K_1 K_2}}{1 + \dfrac{S_o}{K_1}\left(1 + \dfrac{G_o}{K_2}\right)} + \frac{k_{61} + k_{43}\dfrac{S_{in} G_{in}}{K_6 K_5}}{1 + \dfrac{S_{in}}{K_6}\left(1 + \dfrac{G_{in}}{K_5}\right)}, \tag{7}$$

where S_o and G_o are the extracellular and S_{in} and G_{in} are the intracellular substrate concentrations. Expressions for the other three models can be obtained by interchanging the substrate concentrations in f or r in Eq. 7 as appropriate. This result is independent of the small amplitude approximation and is equivalent to that of Wierzbicki et al. (4), although it is more general because it accounts for *trans* substrate effects and two substrates rather than only one. Eq. 7 can be used to predict directly the pre-steady-state relaxation time or the normal mode frequency for a periodic steady-state experiment, regardless of the amplitude of the applied electric field or which state transitions are voltage sensitive.

It is possible to estimate all translocation rate constants for any of the four rapid equilibrium models simply by varying *cis* and *trans* substrate concentrations between extreme limits (0 or ∞) and measuring ω_1 for each condition. Four extreme limits of ω_1 are possible, three of which are linearly independent. Measurement of any three ω_1 and application of detailed balance will yield the four-rate constants. The fourth extreme ω_1 could be measured as a reliability check.

Case 2a: rapid equilibrium, ordered substrate binding in which only the membrane translocation steps are voltage sensitive

The normal mode frequency for each of the four alternative models is easily predicted for the periodic steady-state experiment using the small amplitude approximation. Applying Eq. 6 of Astumian and Robertson (7) to Eq. 7, the normal mode frequency for Case 2a is given by:

$$\omega_1 = [f_o \exp(-ZF\Psi_{DC}/RT) + r_o \exp(+ZF\Psi_{DC}/RT)] \cdot I_0(\alpha), \quad (8)$$

where $I_0(\alpha)$ is the modified Bessel function of the first kind of order zero and α is defined in Eq. 4. ω_1 will have a quadratic dependence on Ψ_{AC} when $\alpha < 1$ since $I_0(\alpha) \approx 1 + \alpha^2/4$ (7, 15). f_o and r_o are model-specific expressions for f and r evaluated at $\Psi_{DC} = 0$ and correspond to those in Eq. 7 for *S*-first binding with mirror symmetry. An expression for the normal mode amplitude could also be written but little can be learned from it due to its algebraic complexity.

It can be shown by application of Eqs. 8, 17, and 36 of Astumian and Robertson (7) that the extra influx (Eq. 6) at infinite frequency, F_∞, is $100[I_0(\alpha) - 1]$. This limit can change only if Ψ_{AC} is changed. F_∞ is the same for each of the four alternatives. Since F_∞ is positive definite, it follows that an AC field will always stimulate influx at high frequencies for Case 2a. This simple result also means that the charge parameter Z can be determined easily by measuring F_∞ as a function of Ψ_{AC}.

Curve A of Fig. 4 shows a typical frequency response for the rapid equilibrium model. It was calculated using the general algorithm. All computations for this case gave seven normal modes but only one normal mode of significant magnitude whose frequency was within 14% of that predicted by Eq. 8. All simulations of the four rapid equilibrium alternatives for Case 2a gave curves qualitatively similar to curve A, having the same high frequency limit as predicted. Differences among models are quantitative only, including differences in ω_1 and the low frequency limit of the extra flux. The latter is sensitive to all variables that are under experimental control. Its magnitude range was ±20% of the DC flux. Low frequencies may either inhibit or stimulate influx relative to the DC influx, depending on experimental conditions. Quantitative differences in low frequency limits also arise among the four alternative models for the same experimental conditions. Deviations of a specific model from experimental data should be detected most easily at low frequencies.

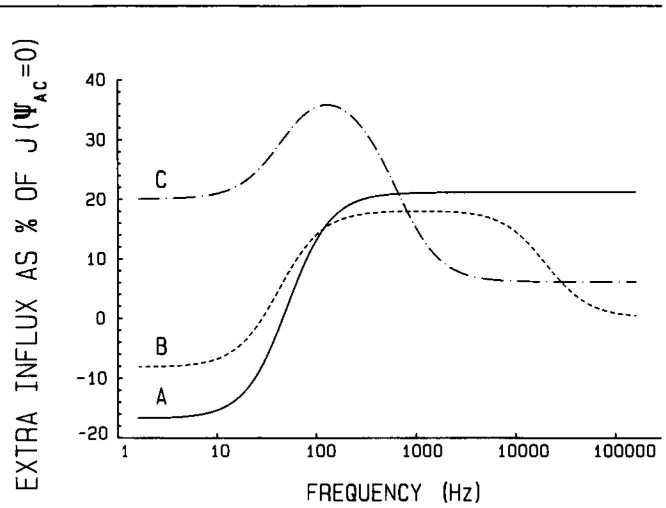

FIGURE 4 Frequency responses of six-state, electroneutral, ordered substrate binding models. The extra AC influx of tracer substrate G due to the AC field (Eq. 6) is plotted as in Fig. 2. Ψ_{AC} was chosen in each case so that $|\alpha| = 0.9$ (Eq. 4). Substrate concentrations for all cases are the same: $[S]_o$ = 100 mM, $[G]_o$ = 0.02 mM, $[S]_{in}$ = 0, $[G]_{in}$ = 0. (*Curve A*) Case 2a. *S*-first, rapid substrate binding, mirror symmetry, only translocation steps are voltage sensitive. The charge parameter $Z_{16} = Z_{34} = Z$ and $Z_{43} = Z_{61} = -Z$. All other $Z_{ij} = 0$. $Z = 0.5$, Ψ_{AC} = 45 mV, and Ψ_{DC} = 0. (*Curve B*) Case 2b. *S*-first, rapid, voltage-sensitive binding of only extracellular substrate G. Translocation steps are voltage insensitive. The charge parameter $Z = Z_{23} = -Z_{32}$. All other Z_{ij} = 0. Z = 0.25, Ψ_{AC} = 90 mV, and Ψ_{DC} = 0. (*Curve C*) Case 3. *S*-first binding, mirror symmetry, "slow" G binding. Only translocation steps are voltage sensitive, and the charge parameters are defined as in *curve A*. Ψ_{AC} = 45 mV and Ψ_{DC} = −45 mV.

Case 2b: voltage-sensitive, *S*-first, ordered rapid binding with mirror symmetry in which membrane translocation steps are not voltage sensitive

A rapid equilibrium condition is not strictly possible for this case because the binding could be slowed significantly by the applied field. Extracellular G binding is assumed sensitive to Ψ_m. Only the equilibrium association constant K_2 would be voltage-sensitive in this case.

If we let the system be rapid equilibrium in the absence of a periodic field, then the first normal mode frequency can be estimated by application of the small amplitude restriction to Eq. 7 or its three other versions. The magnitude of the first normal mode may not always be significant and may not be seen experimentally for all conditions, but simulations show that if several normal modes are of significant magnitude, then the set will always include the first.

Analysis of Eq. 6 for this case, using the rapid equilibrium assumption, gives $F_\infty = 0$. This limit applies only if there is equal apportionment of charge to the association and dissociation binding steps. The limit is not strictly valid because at very high frequency the substrate binding steps can not be at equilibrium. However, all simulations show that F_∞ is very small.

Curve B of Fig. 4 shows that the frequency response of this model differs considerably from Case 2a. Responses tend to have at least two observable normal modes and can have plateaus that are about two decades wide. The low frequency limit is very sensitive to the translocation rate constants and to variables subject to experimental control. The most significant responses in Case 2b occur when the *cis* concentration of G is small. A small G would result in a small pseudo-first-order rate constant and make the binding rate comparable with the translocation rate but highly variable in the presence of a periodic voltage. Multiple normal modes would be readily observable at small G. The results also show that frequency responses should be measured over four or more decades to detect normal modes arising from voltage sensitive binding.

Case 3: partial rapid equilibrium, ordered, S-first substrate binding with mirror symmetry

Only translocation steps are Ψ_m sensitive. It is assumed that the S binding step is very fast but that G binds too slowly for a rapid equilibrium approximation. Rate constants k^0_{23}, k^0_{32}, k^0_{45}, and k^0_{54} of Fig. 3 were each reduced by a factor of 100 for this simulation, whereas all other parameters were unchanged, so that binding rates of substrate G would be comparable with translocation rates. Results cannot generally be described by a single Lorentzian term in Eq. 5. When $\Psi_{DC} = 0$, frequency response curves are qualitatively similar to curve A, but there is no general high frequency limit. F_∞ can provide additional information about the model. When Ψ_{DC} is not zero, several normal modes are introduced, whereas the magnitudes of the flux frequency responses can be increased considerably relative to those for Case 2a. Curve C of Fig. 4 is a typical frequency response. It has a prominent maximum, with three significant normal modes. The peak is narrower than those seen for voltage-sensitive binding. The qualitative behavior of the response changes dramatically as binding rates are slowed further relative to translocation rates, with the extra flux changing to a monotonic decreasing function of frequency.

The *trans* effects are very strong for this model, especially when translocation rate constant asymmetry is introduced by making Ψ_{DC} different from zero. Differences among *trans* effect curves at the same Ψ_{DC} would be observable, whereas repeating the experiments at another Ψ_{DC} could change both the magnitudes of the responses and the shapes of the curves. The frequency responses always differ qualitatively from those for Case 2a and can be much larger with narrower peaks and stronger *trans* substrate effects than for Case 2b.

DISCUSSION

Study of dynamic processes in the frequency domain never achieved prominence in membrane biophysics because it was thought that interpretation of results was strictly model dependent. Robertson and Astumian (8) have shown that under small amplitude restrictions, the Lorentzians that describe the frequency response of any cyclic reaction are true dynamic properties of the system and are independent of any model. Specific models must be able to predict the Lorentzian parameters. This article has extended their work by showing that steady-state frequency response studies may yield considerable new information about membrane transport processes. At the very least, one can obtain an estimate of transporter turnover. The simulations are model specific, of course, but serve to show that frequency response experiments are feasible when applied to some familiar transport systems and models. Frequency responses of radioactive Na and Rb fluxes through the Na^+/K^+ pump in red blood cells have been measured (11) that revealed very interesting and large effects even under the extreme conditions of no ATP, low temperature, and the presence of only one ion substrate at a time. Interpretation of these results in terms of the Post-Albers model was not possible because too few experiments were done, but the results clearly demonstrated the remarkable efficiency of the transporter for capturing the energy in the applied electric field and the existence of a measurable steady-state flux frequency response.

Work with the Na/glucose cotransporter (10, 12) has shown how steady-state and transient data can be used to estimate rate constants. It also shows that transient measurements can be difficult and of limited scope even when the transporter mechanism is electrogenic and has voltage-sensitive substrate binding. There is no detectable transporter current transient when glucose is present (12), whereas the spectrum of normal modes outlined above requires the presence of glucose. The frequency response method could supply new information. The transient experiments in the presence of glucose were done from a holding potential of −50 mV (12), where simulations predict a null frequency response (Fig. 2 *A*). Repeating the transient experiments, in the presence of glucose, from a holding potential of +20 mV might uncover at least the two slower transporter relaxations predicted by the simulation.

Simulations of the Wright group's model show distinctive, large amplitude frequency responses of the tracer fluxes. Responses should be readily measured, could yield more reliable estimates of rate constants than are possible with transient data, and could serve to critically test the model. Measurement of tracer fluxes in a single *Xenopus* oocyte may not yield accurate flux data, but the experiments could be done with multiple cells or with a different cell preparation such as transfected COS-

7 cells (16). Voltage clamp is not required for these studies. The periodic membrane potential could be imposed via an external field, with the amplitude of the transmembrane potential calculated from the Schwan equation (17, 18).

It is possible that periodic membrane potentials with frequencies up to 200 or 300 Hz could be imposed in the *Xenopus* oocyte by voltage clamp. Measurement of the AC current, followed by averaging of the current over one period, would ideally eliminate the capacity transient and might enhance the signal to noise ratio considerably. This approach might permit study of the frequency response without resort to isotopic tracer methods. The normal mode frequencies of the average current should not differ markedly from those of the tracer flux.

The predicted magnitudes of the frequency responses for the extreme case of a nonelectrogenic system show that data of good quality are required to measure them reliably. Use of normalized fluxes like Eq. 6 should enable measurements in many different cell preparations. The internally dialyzed giant axon or barnacle muscle preparations are especially suited for frequency response experiments because each cell serves as its own control and intracellular composition can be controlled in a true steady state. The fact that a modest change in a single rate constant of a model can cause a significant change in the predicted frequency response means that order of magnitude errors in rate constant guesses should be detected easily.

Frequency responses also can be used to choose among models whose differences are subtle, as in mirror and glide symmetry and substrate binding order. The fact that three sets of variables (Ψ_{DC}, *cis,* and *trans* substrate concentrations) can be manipulated independently means that a large number of independent frequency response experiments can be done. Eq. 8 demonstrates explicitly how variations of experimental conditions will affect the frequency response of a specific model. The expressions for ω_1 show that the four alternative models could be distinguished by measuring the *cis* and *trans* substrate effects on ω_1 using protocols much like those used in standard DC steady-state experiments. The dynamic experiments do have the advantage of permitting either the *cis* or *trans* effects to be emphasized simply by changing the Ψ_{DC}. These, combined with DC steady-state flux-substrate activation and Ψ_{DC}-dependence studies, could provide more than enough data for reliable independent estimation of all rate constants with their voltage dependencies for a specific transport model as well as for selection of the best among alternative models.

It is very interesting that the simulations of both the hypothetical six-state model and the Na/glucose cotransporter show that much of the quantitatively important information in a typical tracer flux frequency response should be found at relatively low frequencies. Recall that the zero frequency limit of the Fourier series representation of a function is not necessarily equal to the DC limit. Even though the membrane translocation rate constant k^0_{34} for the hypothetical model is $1000\ s^{-1}$, most observable normal mode frequencies would lie in the range of 10 Hz to 20 kHz. These frequencies are easily achieved, with frequencies below 1 kHz achievable using a voltage clamp in some preparations (19). If transporter turnover is more typical, say $10\ s^{-1}$, then the predicted frequency response range would be 0.1–200 Hz. The low predicted normal mode frequencies of the Na/glucose cotransporter are a consequence of the small translocation rate constant $k^0_{34} = 50\ s^{-1}$. The large capacity transient in the *Xenopus* oocyte preparation would obscure voltage step transients associated with higher frequencies, but steady-state AC fields with frequencies in this range could be applied easily.

I thank Dean Astumian for very helpful discussions and E. Wright for providing preprints of references 10 and 12.

Received for publication 12 May 1992 and in final form 9 September 1992.

REFERENCES

1. Eigen, M., and L. DeMaeyer. 1974. Theoretical basis of relaxation spectrometry. *In* Techniques of Chemistry, VI. 3rd ed. G. G. Hammes, editor. Wiley-Interscience, New York. 63–146.
2. Stark, G., B. Ketterer, R. Benz, and P. Läuger. 1971. The rate constants of valinomycin-mediated ion transport through thin lipid membranes. *Biophys. J.* 11:981–994.
3. Roy, G., W. Wierzbicki, and R. Sauvé. 1991. Membrane transport models with fast and slow reactions: general analytical solution for a single relaxation. *J. Membr. Biol.* 123:105–113.
4. Wierzbicki, W., A. Berteloot, and G. Roy. 1990. Presteady-state kinetics and carrier-mediated transport: a theoretical analysis. *J. Membr. Biol.* 117:11–27.
5. Läuger, P., and P. Jauch. 1986. Microscopic description of voltage effects on ion-driven cotransport systems. *J. Membr. Biol.* 91:275–284.
6. Tsong, T. Y., and R. D. Astumian. 1986. Absorption and conversion of electric field energy by membrane bound ATPases. *Bioelectrochem. Bioenerg.* 15:457–476.
7. Astumian, R. D., and B. Robertson. 1989. Nonlinear effect of an oscillating electric field on membrane proteins. *J. Chem. Phys.* 91:4891–4901.
8. Robertson, B., and R. D. Astumian. 1991. Frequency dependence of catalyzed reactions in a weak oscillating field. *J. Chem. Phys.* 94:7414–7419.
9. Robertson, B., and R. D. Astumian. 1992. Interpretation of the effect of an oscillating field on membrane enzymes. *Biochemistry.* 140:138–141.
10. Parent, L., S. Supplisson, D. D. F. Loo, and E. M. Wright. 1992. Electrogenic properties of the cloned Na^+/glucose cotransporter. II. A transport model under nonrapid equilibrium conditions. *J. Membr. Biol.* 125:63–79.

11. Liu, D-S., R. D. Astumian, and T. Y. Tsong. 1990. Activation of Na^+ and K^+ pumping modes of (Na, K)-ATPase by an oscillating electric field. *J. Biol. Chem.* 265:7260–7267.

12. Parent, L., S. Supplisson, D. D. F. Loo, and E. M. Wright. 1992. Electrogenic properties of the cloned Na^+/glucose cotransporter. I. Voltage-clamp studies. *J. Membr. Biol.* 125:49–62.

13. Hille, B. 1992. Ionic Channels of Excitable Membranes. 2nd ed. Sinauer Assoc. Inc., Sunderland, MA. 607 pp.

14. Lowe, A. G., and A. R. Walmsley. 1987. A single turnover of the glucose carrier of the human erythrocyte. *Biochim. Biophys. Acta.* 903:547–550.

15. Abramowitz, M., and I. A. Stegun. 1964. Handbook of Mathematical Functions. U.S. Department of Commerce, Washington, DC. 1046 pp.

16. Birnir, B., H.-S. Lee, M. A. Hediger, and E. M. Wright. 1990. Expression and characterization of the intestinal Na^+/glucose cotransporter in COS-7 cells. *Biochim. Biophys. Acta.* 1048:100–104.

17. Tsong, T. Y. 1990. Electrical modulation of membrane proteins: enforced conformational oscillations and biological energy and signal transductions. *Annu. Rev. Biophys. Biophys. Chem.* 19:83–106.

18. Vellick, F., and M. Gorin. 1940. The electrical conductance of ellipsoids and its relation to the study of avian erythrocytes. *J. Gen. Physiol.* 23:753–771.

19. Palti, Y., and W. J. Adelman Jr. 1969. Measurements of axonal membrane conductances and capacity by means of a varying potential control voltage clamp. *J. Membr. Biol.* 1:431–458.